

THE SIZE EFFECT AND X-RAY FLUORESCENCE SPECTRA OF METALLIC NANOPARTICLES

Yu.E. Kolyada¹, N.A. Savinkov², A.A. Bizyukov³, O.N. Bulanchuk²

¹Mariupol State University, Mariupol, Ukraine;

²Donetsk State University of Management, Mariupol, Ukraine;

³V.N. Karazin Kharkiv National University, Kharkov, Ukraine

E-mail: yukol@ukr.net

X-ray fluorescence scattering spectra of metallic nanoparticles (copper (Cu), aluminum (Al), titanium (Ti)) are studied. Nanostructures were fabricated by nonequilibrium metallic vapor-induced desorption from plasma blob which was generated by pulse electrothermal plasma accelerator. It is discovered the shift of X-ray spectra on depending of particle sizes. The shift of X-ray fluorescence scattering spectra for K_{α} - and K_{β} -lines is registered for Al nanostructures with average size ≈ 14 nm. The analogical shift is not observed for Ti and Cu particles with greater size.

PACS: 78.70.En, 81.16.-b

INTRODUCTION

At last decades the explosive development of nanotechnologies and related new scientific tendencies are under high interest for researching of metallic nanoparticles and nanostructures which demonstrates unique electrophysical and optical properties that is not typical for isolated atoms or solid state metals [1-3]. These properties are the basis for production of nanocomposite metallic coatings [4, 5], the manufacturing of emitters and cathode components of electronic devices using nanostructured materials [6], the construction of nanoscale carbon materials – fullerenes and nanotubes [7].

It is known that changing of size and shape of nanoparticle alters its electronic structure and optical properties (size effect). The size effect arises in many experimental researches. The intensity dependencies of gold cluster photoluminescence on number of atoms in cluster are shown in [8,9]. It was researched the optical Raman scattering spectra of the nanocrystals (with particle size 5 nm) [10].

It is theoretically proved that main maximum of optical Raman scattering spectra in frequency range (500...520) cm^{-1} displaces significantly to lower energy for nanostructures with a smaller size. For nanoclusters of transition metals (Ni, Co, Cr) it is experimentally observed the shift of photoelectron spectra and "core" electrons binding energies in atoms in dependence of nanoclusters size [11].

Now the investigation of nanoparticles X-ray spectra is under the great interest because it is insufficiently understood. Particularly the X-ray shifts of manganese K-lines are obtained for nanoparticles oxides MnO , Mn_3O_4 and MnO_2 relatively to the corresponding macro material [12]. However in mentioned above references and many analogical works the electromagnetic properties of small particles were researched only for particles with a size less than 10 nm

The purpose of the work is the investigation of X-ray nanoparticles (Cu, Al, Ti) fluorescence scattering spectra and making comparison it with macro materials spectra.

1. EXPERIMENTAL DEVICE

The electrothermal plasma accelerator (ETPA) (Fig. 1) is used for metallic nanoparticles production.

ISSN 1562-6016. BAHT. 2017. №1(107)

PROBLEMS OF ATOMIC SCIENCE AND TECHNOLOGY. 2017, № 1. Series: Plasma Physics (23), p. 179-182.

The body 1 is made of dielectrical rigid thick-walled tube with length 40 sm. The inner diameter is 8 mm and wall thickness is 1 sm. The edge of dielectrical body is molded by metallic barrels 3 and 4. The changeable rod cathode 2 with diameter 6 mm is attached to the barrel 3 by means of threaded connection. The cathode is made of ETPA and its application in some scientific researches is shown in [13, 14].

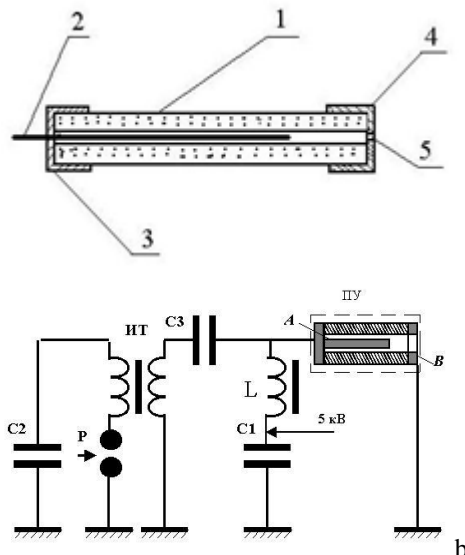


Fig. 1. The electrothermal plasma accelerator (a) and its electrical power supply circuit (b)

2. EXPERIMENTAL RESULTS

For collecting and analysis of nanoparticles are used glass substrates with size (3 x 3) sm positioned outside of the ring anode 4 on the distance of (6...8) sm. The investigation of nanoparticles shapes and sizes was carried out by a scanning electron microscope JSM - 6390LV (JEOL company, Japan). On one photo there are 200...400 particles of different sizes [15].

By using a such method of plasma blob generation there are atoms and molecules of wall material, electrodes and air in it. This can result to oxides, nitrides and hydrocarbon groups formation. In the combustion product of high-current discharge arc it is possible the existence and ejection of a droplet fraction of the cathode material. Just the cathode is the most affected to

erosion in the discharge. For the clearing of nanoparticles generation mechanism the chemical composition of synthesized particles is studied. The method of X-ray fluorescence spectral analysis (XRF) is used. The measurements are made by wave X-ray fluorescence spectrometer ARL OPTIM'X-0335 (spectral resolution ≈ 15 eV for the emission K_α and K_β lines). It was carried out the quantitative spectral analysis of the nanoparticles deposited on the glass substrates and on the cathode material (macro material). Then the elemental composition of macro material was compared with the material composition of the synthesized nanostructures.

In the Table the results of such comparison for aluminum cathode are presented (the percentage ratio by components weight). Table shows that the composition by percentage of the same elements for the cathode macro material and for the aluminum nanoparticles synthesized on substrates is essentially different. It is important to note that the series of elements (W, Pb, Ga, Zn) inherent to initial aluminum cathode is fully absent in the nanoparticles composition. The analogous regularity is also characteristic for the titanic and copper cathode used in the study. Thus the synthesis of nanoparticles under our experiment occurs not due to the "spray" of cathode material droplets but exclusively as the result of the non-equilibrium condensation of supersaturated metal vapor from the discharge region onto the substrate. It is not detected oxides, nitrides and other compounds that could theoretically arise in the discharge.

The elemental composition of the aluminum nanoparticles on glass (right column), the material of the aluminum cathode (center column) and glass substrate (left column)

Element	glass, m/m %	aluminum, m/m %	Al on glass, m/m %
Si	66.43817	0.421	61.2706138
Na	16.73793	0.0445	11.83023801
Ca	8.064639	0.0595	7.572123027
Mg	4.945297	0.304	3.737892792
Al	2.168323	98.55	13.8725918
K	1.004276	0.0099	0.942180193
S	0.368995	0.064	0.418104503
Fe	0.125915	0.352	0.134101721
Cl	0.079505	0.0435	0.144891514
Px	0.017499	0.0783	0.026974484
Ti	0.015977	0.0062	0.014450616
Cu	0.014836	0.0181	0.01657004
Zr	0.005706	–	0.005780247
Rb	0.003804	–	0.004238847
Ni	0.003233	0.0049	0.002312099
Sr	0.003043	–	0.001926749
Mn	0.002853	0.0034	0.005009547
W	–	0.0114	–
Pb	–	0.0104	–
Ga	–	0.0082	–
Zn	–	0.0071	–
–	100	99.9964	100

In [16] it was calculated the sizes and was carried out the statistical analysis of microscopic cathode material particles arisen in the pulse high-voltage vacuum discharge. The good correlation between mean free path of Fermi-electrons in corresponding metal and characteristic size of the aerosol microparticles follows from obtained data. This feature is characteristic for pulsed heat system.

This is why in this study we used the analogous technique: the sample mean of nanoparticles sizes for used cathodes is calculated by known ratio of mean free path of Fermi-electrons $\langle \lambda_F \rangle = Ed_0 / \pi n_0 kT$ (where E – Young modulus; d_0 – lattice constant; n_0 – free-electron concentration in the metal which is determined by value of Hall constant; k – Boltzmann constant; T – absolute temperature). For Al: $\langle \lambda_F \rangle = l_{Al} = 14$ nm; for Cu: $\langle \lambda_F \rangle = l_{Cu} = 30.1$ nm and for Ti: $\langle \lambda_F \rangle = l_{Ti} = 85.9$ nm. The calculated particle sizes are in a good agreement with the sizes observed by the electron microscope. The X-ray fluorescence spectra are investigated for aluminum, copper, titanic nanoparticles made by a such method. For this purpose the X-ray fluorescence spectrometer ARL OPTIM'X-0335 (rhodium node) was used. Radiation of Rh K_α ($h\nu \approx 20213$ eV) and Rh K_β ($h\nu \approx 2276$ eV) lines are applied for the fluorescence excitation. Fig. 2 shows these spectra which are compared with the spectra of cathode macro material. On Fig. 2,a,b the fluorescence spectrum of the aluminum nanoparticles has the energy shift with respect to the spectrum of macro material. The shift of K_α line is $\Delta E \approx 0.35$ eV and K_β line shift is $\Delta E \approx 3.81$ eV. The analogues shift for titan and copper is not observed. In this case the both lines coincide (Figs. 2,c and 2,d).

3. DISCUSSION

The obtained spectra can be explained as follows. It is known that even small changes in the size of the nanoparticles lead to a visible shift of the optical absorption band of nanomaterials. This results to their wide application in optics. Distributed in a transparent matrix metallic nanoparticles with size $l < 20$ nm reveal unusual optical properties. One example of such systems are known even in ancient times colored glass and stained glass windows of medieval Gothic cathedrals (which are colloidal solutions of metal clusters in a glass matrix) [17]. According to classical optics the absorption spectrum of colloidal solution doesn't depend on particles size when cluster size D is substantially smaller than the wavelength of incident light: $D/\lambda \ll 1$. Thus the radiation absorption of material doesn't depend on the nanoparticles size for a nanosize (10...100 nm) systems and wavelengths in the optical spectrum. But it is supposed that experimentally registered radiation absorption in the metallic nanoparticles systems occurs due to the size effect associated with the plasmon resonance absorption. The obtained results exhibit that caused by localized plasmons size effect appears in the fluorescence X-ray spectrum of metallic nanoparticles also. Unlike the optical spectra in this case there is resonance absorption of the initial X-ray photons

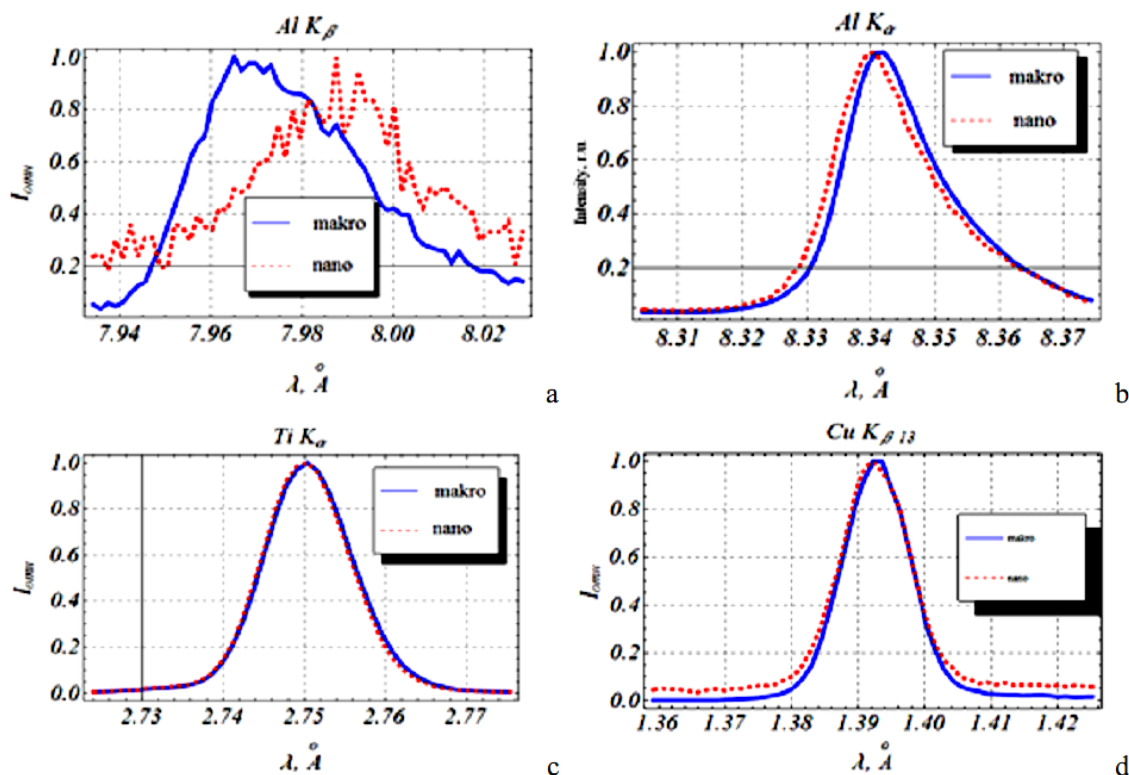


Fig. 2. X-ray spectra of the nanoparticles fluorescence and corresponding macro material: aluminum K_{α} (a) and K_{β} -line (b) (dashed curve – nanoparticle; solid curve – macro material); titanium (both curves coincide) (c); copper (both curves coincide) (d)

by K-shell electrons of aluminum atoms (likewise copper and titanium atoms). As a result a vacancy appears in the atomic K-shell. On the next stage the vacancy is filled by the electrons of L-shell (L→K-transition) which leads to the K_{α} lines emission by the aluminum atoms (see Fig. 2,a) and titanium atoms (see Figs. 2,c,d). In the Al and Cu atoms the vacancy is also filled by electrons of M-shell ($M_{2,3}$ →K-transition) that leads to the K_{β} emission line (aluminum – Fig. 2,b) and $K_{\beta 13}$ lines (copper – Fig. 2,d). Under radiation absorption of initial X-rays quanta and simultaneously under fluorescence excitation processes it also can occur radiationless transitions of electrons, $L I \rightarrow L III$ and $L I \rightarrow L III_{MV}$ – transitions leading to the release of photoelectrons and Auger electrons from atoms. The part of the initial X-ray photon energy is consumed by these processes. The energy decrease of the registered fluorescence quanta in comparison to the energy of the initial X-ray photons indicates on this fact. The energy peaks of the spectral curves Al K_{β} on Fig. 2,b are in $\approx (14 \dots 15)$ times less than the energy of the initial emission line of a rhodium anode. The energy peaks of the spectral curves for titanium and copper are less than the energy of the initial emission line in ≈ 5 times and ≈ 2.55 times respectively.

The spectra shift of Al nanoparticles with respect to the aluminum solid (K_{β} – line is shifted to lower energies, the K_{α} line – to the high-energy region – Fig. 2,b,a) indicates to the energy level deformation (K-, L- and M-levels) of the aluminum atom "core" electrons under formation process of nanostructures with the particle size of smaller than a some critical size.

For aluminum nanoparticles with size $l = 14$ nm such deformation takes place and it is not visible for larger nanoparticles: titanium $l = 85.9$ nm and copper $l = 30.1$ nm.

This deformation is so small that it can't appear in the optical spectra. On the Fig. 2,b the shift of the two curves maximum for the K_{β} -line is $\approx 0,023$ Å that is much smaller than the wavelength of the visible range.

Thus in this paper it is proposed a completely new approach to the study of the metallic nanostructures properties by using of X-ray fluorescence spectra for the size and structural analysis of metal nanoparticles.

CONCLUSIONS

1. It is synthesized the aluminum, titanium and copper nanoparticles onto dielectric substrates by using ETPA. The fulfilled X-ray spectral analysis (RFA) allows to determine the mechanism of nanoparticle synthesis using technique of the non-equilibrium supersaturated condensation of the plasmoid metal vapor onto the substrate.
2. The X-ray fluorescence spectra of aluminum, copper and titanic nanoparticles deposited on the dielectric substrates are experimentally obtained and analyzed. These spectra are compared with the spectra of the macro materials of corresponding cathodes.
3. It is found the size effect of the X-ray fluorescence spectra: the fluorescence spectra of aluminum nanoparticles (K_{α} and K_{β} line) are shifted with respect to corresponding spectrum of macro material. There is no such spectral line shift for Ti and Cu nanoparticles with larger size.

REFERENCES

1. S.A. Maier. *Plasmonics: Fundamentals and Applications*. New York: "Springer", 2007, p. 201.
2. S.V. Gaponenko. *Introduction to Nanophotonics*. Cambridge: "Cambridge University Press", 2010, p. 465.
3. A.I. Gusev. *Nanomaterials, nanostructures, nanotechnology*. Moscow: "Fizmatlit", 2009, p. 416 (in Russian).
4. S.V. Eliseeva, Yu.F. Nasedkina, D.I. Semenzov. Optical spectra of nano composite medium and films with metallic inclusions // *Optics and Spectroscopy*. 2014, v. 117, № 6, p. 914-920.
5. M.A. Yarmolenko, A.A. Rogachov, P.A. Luchnikov, A.B. Rogachov. Preparation of film coatings based on a polymeric matrix with silver nanoparticles by vapor deposition // *Nanomaterials and nanostructures – XXI century*. 2012, № 2, p. 21-25.
6. N.N. Balan, E.I. Ivaschov, P.A. Luchnikov, A.B. Nevskiy. Technological features of the formation of the cathode parts of field-emission and tunneling nano- and microdevices // *Nanomaterials and nanostructures – XXI century*. 2012, № 2, p. 36-43.
7. V.V. Klimov. Nanoplasmonika // *Uspehi Phisicheskikh Nauk*. 2008, v. 178, № 8, p. 875-880 (in Russian).
8. J. Zheng, C. Zhang, R.M. Dickson. Highly fluorescent, water-soluble, size-tunable gold quantum dots // *Physical Review Letters*. 2004, v. 93, № 7, p. 077402-1–077402-4.
9. J.I. Gonzalez, T.-H. Lee, M.D. Barnes, Y. Antoku, R.M. Dickson. Quantum mechanical single-gold-nanocluster electroluminescent light source at room temperature // *Physical Review Letters*. 2004, v. 93, № 14, p. 147402-147405.
10. V.G. Kravets. Silicon nanoparticles: photoluminescence, the complex refractive index and their relationship with the band structure // *Optics and Spectroscopy*. 2013, v. 114, № 2, p. 253-259 (in Russian).
11. V.D. Bormann, M.A. Pushkin, V.N. Tronin, V.I. Troyan. A study of the evolution of the electronic properties of transition metals nanoclusters on the graphite surface // *Experimental and Theoretical Physics Journal*. 2010, v. 137, № 6, p. 1151-1174.
12. A.A. Naberezhnov, A.A. Petrunin, A.E. Sovestnov, D.A. Kurdyukov, E.V. Fomin, S.B. Vahrushev. Shifts of X-ray lines of manganese in its oxide nanoparticles // *Journal Technical Physics Letters*. 2015, v. 41, № 24, p. 89-94.
13. Yu.E. Kolyada, V.I. Fedun. Pulse electrothermal Plasma Accelerators and its Application in scientific Researches // *Problems of Atomic Science and Technology. Series "Plasma Electronics and New Methods of Acceleration"*. 2015, v. 98, № 4, p. 325-330.
14. Yu.E. Kolyada, V.I. Fedun. Excitation of elastic pulses by powerful plasmoids in the acoustic waveguide // *Problems of Atomic Science and Technology. Series "Plasma Electronics and New Methods of Acceleration"*. 2008, v. 56, № 4, p. 260-263.
15. Yu.E. Kolyada, V.I. Fedun, V.I. Tyutyunnikov, N.A. Savinkov, A.E. Kapustin. Formation Mechanism of the Metallic Nanostructures Using Pulsed Axial Electrothermal Plasma Accelerator // *Problems of Atomic Science and Technology. Series: "Plasma Electronics and New Methods of Acceleration"*. 2013, v. 86, № 4, p. 297-300.
16. Yu.E. Kolyada, V.I. Fedun, S.P. Desyatsky. Statistical analysis of the droplet fraction of explosion-emission cathode // *Problems of Atomic Science and Technology. Series "Plasma Electronics and New Methods of Acceleration"*. 2006, № 5, p. 113-115.
17. V.V. Klimov. *Nanoplasmonika*. Moscow: "Fizmatlit", 2009, p. 480 (in Russian).

Article received 29.11.2016

РАЗМЕРНЫЙ ЭФФЕКТ И РЕНТГЕНОФЛУОРЕСЦЕНТНЫЕ СПЕКТРЫ МЕТАЛЛИЧЕСКИХ НАНОЧАСТИЦ

Ю.Е. Коляда, Н.А. Савинков, А.А. Бизюков, О.Н. Буланчук

Исследуются рентгенофлуоресцентные спектры рассеяния металлических наночастиц меди, титана и алюминия. Наноструктуры были получены методом неравновесной десорбции на стеклянную подложку металлического пара из плазменного сгустка. Для этого использовался импульсный электротермический плазменный ускоритель. Анализ рентгеновских спектров позволил обнаружить их смещение по частоте в зависимости от размеров наночастиц. Для наноструктур Al, имеющих средний размер ≈ 14 нм, зафиксирован сдвиг рентгенофлуоресцентных спектров рассеяния для K_{α} - и K_{β} -линий. Аналогичный сдвиг отсутствует для частиц титана и меди, имеющих больший размер наночастиц.

РОЗМІРНИЙ ЕФЕКТ І РЕНТГЕНОФЛУОРЕСЦЕНТНІ СПЕКТРИ МЕТАЛЕВИХ НАНОЧАСТИНОК

Ю.Є. Коляда, М.О. Савінков, О.О. Бізюков, О.М. Буланчук

Досліджуються рентгенофлуоресцентні спектри розсіювання металевих наночастинок міді, титану та алюмінію. Наноструктури було виготовлено методом нерівноважної десорбції на скляну підкладку металеві пари із плазмового згустка. Для цього використовувалася імпульсний електротермічний плазмовий прискорювач. Аналіз рентгенівських спектрів дозволив встановити їх зміщення по частоті в залежності від розмірів частинок. Для наноструктур Al, що мають середній розмір ≈ 14 нм, зареєстровано зміщення рентгенофлуоресцентних спектрів розсіювання для K_{α} - та K_{β} -ліній. Аналогічне зміщення відсутнє для частинок титану та міді з більшими розмірами.